Design of a Multi-Cell Superconducting Cavity for the Cornell ERL Main Linac

Michael P. Antosh

Department of Physics, University of New Hampshire, Durham, NH, 03824

(Dated: August 11, 2006)

The Cornell ERL is a proposed x-ray source. Part of the design of this ERL is the design of the main linear accelerator (linac) by the Superconducting Radio Frequency group at Cornell. One of the main components of this linac is a network of 7-cell superconducting cavities. Each cavity is a resonator that accelerates beams with the electric field of the so-called fundamental electromagnetic mode. However, there are also higher order modes (HOMs) which have negative effects on the beam. In my project, I optimized the shape for the center cells of these cavities with the goal of improving the damping of HOMs and lowering cryogenic losses in the cavity. I also began to design the end cells of the cavity with the same goals, and modeled as a baseline the TESLA cavity shape in the 3 dimensional modeling program Microwave Studio.

I. INTRODUCTION AND THEORY

A superconducting radio frequency (SRF) cavity is an electromagnetic resonator used to accelerate particles. The cavity, made of niobium tin, is kept at very low temperatures, around 1.8 Kelvin, and has high quality factors on the order of 10^{10}. Each cavity is made out of a fixed number of cells that are usually symmetric around a central axis. The 2-dimensional profile of each half cell consists of 2 ellipses, one at the equator (higher part) and one at the iris (lower part). These ellipses are connected by a line tangent to both ellipses (see figure 1). The resonator has a fundamental mode that is used to accelerate the particle, but it also has many higher-order modes (HOMs) that can be excited by the beam and act back harmfully on the beam. These HOMs come in different varieties: monopole modes have no transverse on-axis fields, while dipole, quadrupole, and other multiple-polarization modes have transverse on-axis fields.

Each cavity incorporates 3 cell designs. The middle cell design is used for the middle cells as well as the inner halves of the outermost cells. The outer half of both outermost cells is a freestanding design in itself because of its transition to the beam tubes and its effects on HOM damping. There are 6 free variables in each cell: the 4 radii of the 2 ellipses, the length of cell, and the height of the cell. In the middle cells, the length is required to be the 1/2 wavelength at the accelerating mode frequency, so that the electric field and the particle stay in phase. The height is changed to fix the cell fundamental frequency to the desired value of 1.3GHz. The height of the end cells is fixed by the middle cells, and the length of the end cells is used to tune the frequency.

There are several figures of merit used to evaluate the geometric and performance properties of an SRF cavity. R/Q is a geometric value used to evaluate the coupling between the beam and a cavity eigenmode. High R/Q indicates strong coupling. For a monopole mode[1], R/Q is defined as

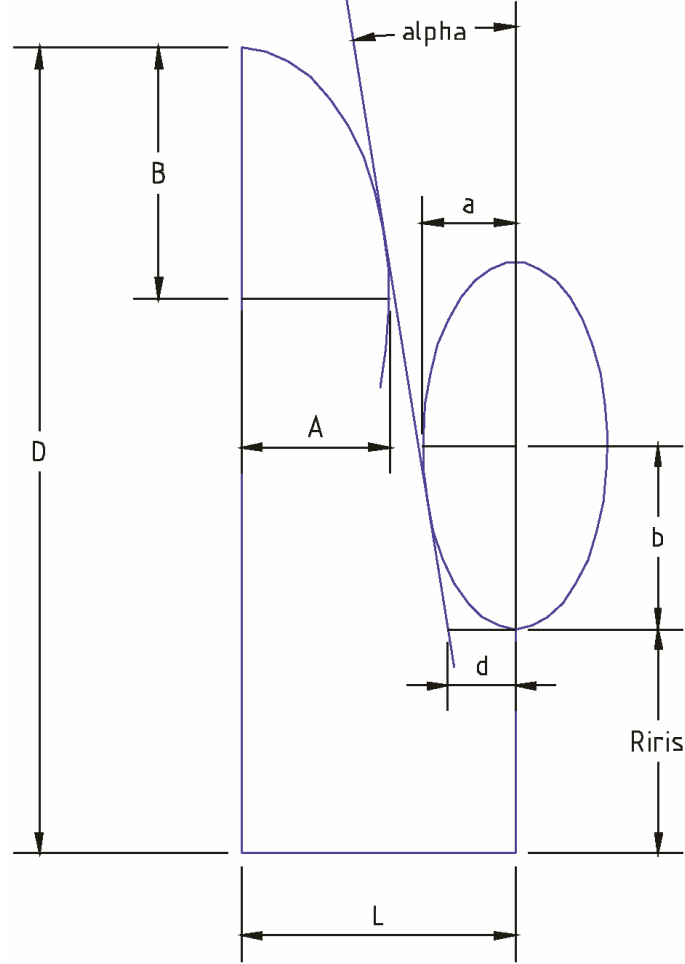$$R/Q_{mode} = \frac{V_c^2}{2 \cdot \omega_{mode} \cdot U} \tag{1}$$

FIG. 1: Geometry of a Half Cell[2]

Where ω is the frequency of the mode, U is stored energy, and V is the accelerating voltage (integral of voltage as seen by the beam)[1]:

$$V_c = \left| \int_0^d E_z(\rho = 0, z) e^{i\omega_{mode} z/c} \cdot dz \right| \tag{2}$$

Similarly, for a dipole mode[1],

$$R/Q_{mode} = \frac{V_c(a)^2}{2 \cdot \omega_{mode} \cdot U \cdot a^2} \tag{3}$$

Where a is the distance off of the symmetry axis at which the voltage is calculated - dipole modes have zero voltage on the axis. Another figure of merit is the quality factor Q, which indicates the overall quality of the eigenmode of the cavity[1]:

$$Q = \frac{\omega_{mode} U}{P_{diss}} \tag{4}$$

Where P_{diss} is the dissipated power. The higher Q, the smaller are the losses of a mode normalized to its stored energy, and the narrower is the width of the ersonance curve of that

cavity mode. A third figure of merit is the geometry factor G. G is defined by[1]

$$G = Q_0 \cdot R_s \tag{5}$$

Q_0 is the quality factor from wall losses, Rs is the surface resistance of the cavity, a frequency dependent material property of niobium[1].

$$R_s = A_s \omega^2 exp(-\frac{\Delta(0)}{k_b T}) + R_0 \tag{6}$$

Where A_s is a material parameter, ω is the frequency, $\Delta(0)$ is half of the energy gap, k_b is Boltzmann's constant, T is the temperature, and R_0 is the residual resistance. I used $R_s = 1.33024 \cdot 10^{-8}\Omega$ in my calculations for the surface resistance of niobium at 1.8K.

The power dissipated in cavity walls from the fundamental mode are given by equation 7[1]:

$$\bar{P}_{fm} = \frac{V_c^2}{R/Q \cdot G} \cdot R_s \tag{7}$$

V_c is 12.9 MV/m for the ERL[3]. This indicates that $R/Q \cdot G$ should be high for the fundamental mode! The maximum power transfer from the beam to a cavity mode happens in resonant excitation, i.e. when the mode frequency in a multiple of the bunch repetition rate ($f_{hom} = N \cdot f_{bunch}$) Because the ERL design involves two beams, the dangerous frequencies are actually multiples of 2.6GHz[3]. The power lost to a resonant monopole HOM is[1]:

$$\bar{P}_{HOM,res} = 2 \cdot R/Q \cdot Q \cdot I^2 \tag{8}$$

where I is the beam current. Thus, a low $R/Q \cdot Q$ for these modes is desired, or a cavity designed such that $f \neq N \cdot f_{res}$. Cell shape design changes $R/Q \cdot Q$.The average power (over many cavities) lost by the beam into HOMs is:

$$\bar{P}_{HOM} = K_{||} \cdot I_b \cdot Q_b \tag{9}$$

I_b is the beam current ($2beams \cdot 100mA$ for the ERL) and Q_b is the bunch charge (77pC for the ERL)[3]. $K_{||}$ is the so-called longitudinal loss factor of the cavity. A small $K_{||}$ is preferable to reduce HOM losses. Loss factor depends on cavity shape and bunch length. Shorter bunch gives a higher $K_{||}$. For the ERL, bunch length is 0.6mm[3]. K introduces the variable of iris radius, because K scales with the iris radius:

$$K_{||,monopole} \propto \frac{1}{r_i}[6] \tag{10}$$

A large iris radius is preferable to minize HOM losses. The so-called transverse loss factor $K_\perp$ scales as

$$K_\perp \propto \frac{1}{r_i^3}[1] \tag{11}$$

and is a measure of the strength of transverse kick modes of a cavity. Again, a large iris radius is preferable to minimize the potential harm of transverse modes.

For a given electron beam, the current at which it beam stability will occur as the result of a transverse mode excited by the beam is inversely proportional to $R/Q \cdot Q_0$[7]:

$$I_{bbu} \propto \frac{1}{R/Q \cdot Q_0} \tag{12}$$

As will be shown later, the shape of the end cells can be optimized such as to minimize A for HOMs, thereby increasing the BBU threshold current and reducing the HOM power of monopole modes in case of resonant excitation.

Also, power losses at low temperature environments cost reqire signifcantly more power for cooling. [5]:

$$\bar{P}_{fm,room} = \bar{P}_{fm} \cdot 800W/W \tag{13}$$

For the fundamental mode losses at 1.8K, about 800W of power are required to intercept 1W at 1.8K. The HOM power will be intercepted at 80K, with a cryogenic efficiency of about 25W/W[5]:

$$\bar{P}_{HOM,room} = \bar{P}_{HOM} \cdot 25W/W \tag{14}$$

Minimizing $\bar{P}_{fm}$ gives the design goal of maximizing $R/Q \cdot G$ for the fundamental mode, especially in the center cells since most of the fundamental mode power loss will occur there.

II. MICROWAVE STUDIO AND CLANS MODELLING OF THE BASELINE 7-CELL CAVITY

The baseline cavity is 5 TESLA shaped center cells and special end cells with beam tube radii of 53 and 65mm[5]. Microwave Studio[4] is a 3-dimensional modeling program with an electromagnetic eigensolver. I constructed a one-cell model of a TESLA shaped center cell and then the entire 7-cell model. To produce this model, I combined 3D shapes such as cylinders, cones, and stretched toruses. I calculated 20 of the lowest frequency modes for the 7-cell cavity, including monopole and dipole modes. G for any mode can be found from
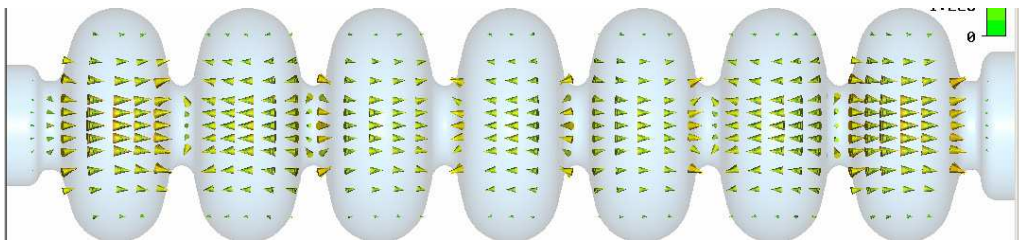

FIG. 2: Fundamental Mode in TESLA Cavity Modelled in Microwave Studio

equation (5) in the introduction. Frequencies were determined using both the AKS and JDM eigenmode solvers in Microwave Studio. R/Q values were determined by measuring the field profile along either the axis of the shape, or along a line parallel to the axis and 0.5 cm away for dipole modes. This field profile was numerically integrated to find the voltage felt by the charge as in equation 2. Next, this voltage was used to find R/Q from formulae 1 and 3 in the introduction. Monopole and dipole modes were recognized by looking at a 2D cross-section of modes in the Microwave Studio results file. Monopole modes have no transverse electric field on axis, while dipole modes do - the different colors on figure 3 for the dipole mode are positive and negative fields that create a transverse field:

A magnetic symmetry plane has been introduced to make the solver's mesh small enough to be managable for a computer. This eliminates one polarization of dipole modes. See table I for these results.

CLANS and CLANS2 are 2-dimensional electromagnetic modeling programs that assume axial symmetry about the r=0 axis. CLANS calculates monopole modes, and CLANS2
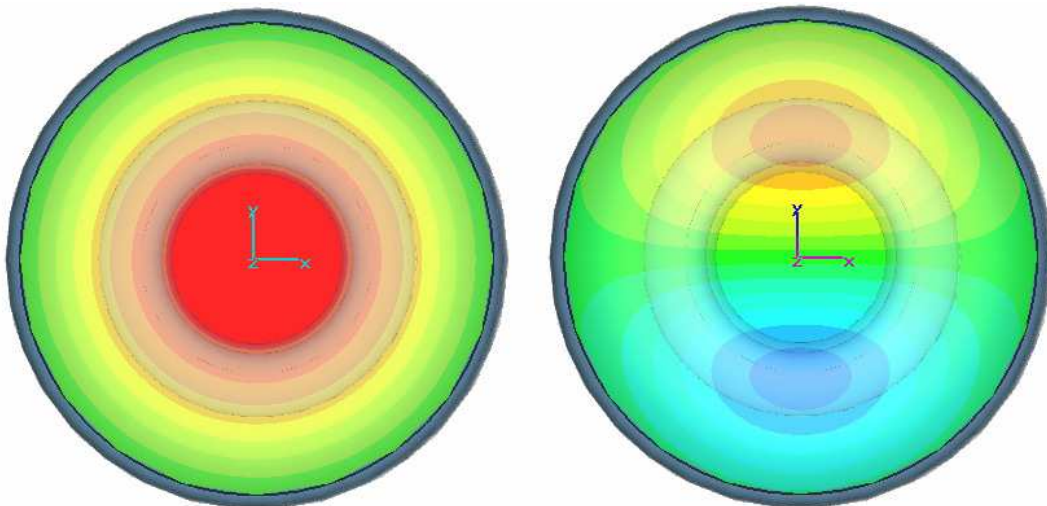
FIG. 3: Microwave Studio Cross-Sections of Monopole (left) and Dipole (right) Modes

calculates dipole modes and modes of higher azimuthal variation (quadrupole modes, etc). These programs are useful because they run significantly faster than 3D codes like Microwave Studio. I modeled the baseline 7-cell cavity and ran simulations for R/Q, G, and frequency of lower frequency modes in order to compare these CLANS results to the Microwave Studio results. As expected, my results in CLANS and Microwave Studio were indeed very similar - see table II. Note that R/Q is much higher for the fundamental mode.

As a measure of the field amplitude in the end tubes of a cavity I studied the following approach: cavity modes have been calculated with both magnetic and electric boundary conditions at the tube ends, and the difference in the mode frequency between the two conditions has been calculated. A high 1/deltaF indicates trapped modes with potentially high Q increases. I calculated this for monopole, dipole, and quadrupole modes (see table III, figure 4). Both monopole and dipole mode comparisons verfied the conclusion that a mode with a high Q also has a small change in frequency between electric and magnetic bound simulations. This happens because a small change between boundary conditions indicates a low field inside the tubes, which likely gives a high Q[5]. In figure 4I compared the axis electric field profiles of two monopole HOMs, one with a delta F on the order of 100 times higher than the other. The mode with the bigger delta F has much more field in the end cells and much less field in the center cells, indicating that it is being propagated much more effectively.

The quadrupole modes were studied in a similar fashion - I determined that these low frequency quadrupole modes propagate into the beam tubes, so that they can be damped by the HOM absorbers between the cavities. Note that even though the delta F is actually smaller for the quadrupole modes, the R/Q values are so small that the quadrupole mode R/Q/delta F values are orders of magnitude smaller than the highest dipole mode R/Q/delta F values.

TABLE I: 20 Mode Microwave Studio Simulation Results, $U = 1J$ Stored Energy

Mode	Frequency[GHz]	V_c[V]	G[Ω]	R/Q[Ω]	Type	V_c, a=0.5cm[V]	R/Q[Ω/cm^2]
1	1.277148649	6.70E+03	2.68E+02	0.0027983	monopole	-	-
2	1.28044956	4.53E+03	2.68E+02	0.0012738	monopole	-	-
3	1.285259348	1.84E+04	2.69E+02	0.0210739	monopole	-	-
4	1.290654835	1.06E+04	2.69E+02	0.0068794	monopole	-	-
5	1.295569034	2.51E+04	2.70E+02	0.0385491	monopole	-	-
6	1.299000291	2.40E+04	2.70E+02	0.0354185	monopole	-	-
7	1.300233275	2.52E+06	2.70E+02	390.17301	monopole	-	-
8	1.375711252	-	2.78E+02	-	tube dipole	3.92E+03	3.55E-03
9	1.549475803	-	2.95E+02	-	tube dipole	1.74E+04	6.21E-02
10	1.621759124	-	3.02E+02	-	dipole	9.50E+03	1.77E-02
11	1.632448216	-	3.03E+02	-	dipole	5.77E+03	6.49E-03
12	1.649889773	-	3.05E+02	-	dipole	2.99E+04	1.73E-01
13	1.672952953	-	3.07E+02	-	dipole	1.33E+04	3.36E-02
14	1.698063314	-	3.09E+02	-	dipole	1.02E+05	1.94E+00
15	1.719489583	-	3.11E+02	-	dipole	1.50E+05	4.18E+00
16	1.745742193	-	3.13E+02	-	dipole	1.66E+05	5.03E+00
17	1.776482823	-	3.16E+02	-	dipole	5.59E+04	5.60E-01
18	1.794933083	-	3.18E+02	-	dipole	7.01E+04	8.72E-01
19	1.819576024	2.04E+05	3.20E+02	1.8227147	tube mono	-	-
20	1.840648986	-	3.22E+02	-	dipole	1.42E+04	3.48E-02

TABLE II: Monopole Mode Comparison, MWS vs. CLANS

Mode	MWS f[GHz]	CLANS f[GHz]	MWS G[Ω]	CLANS G[Ω]	MWS R/Q[Ω]	CLANS R/Q[Ω]
1	1.27715	1.27736	268	264	2.80E-03	2.56E-03
2	1.28045	1.28066	268	264	1.27E-03	1.31E-03
3	1.28526	1.28548	269	265	2.11E-02	1.82E-02
4	1.29065	1.29088	269	265	6.88E-03	6.00E-03
5	1.29557	1.29580	270	266	3.85E-02	2.20E-02
6	1.29900	1.29924	270	266	3.54E-02	7.21E-03
7	1.30023	1.30048	270	266	3.90E+02	3.93E+02

TABLE III: CLANS2 Dipole Similar Frequency Mode Comparison, Odd vs. Even Symmetry Bound

$f_2[GHz]$	$f_3[GHz]$	$\Delta f[GHz]$	$(R/Q)_2[\Omega/cm^2]$	$(R/Q)_3[\Omega/cm^2]$	max $(R/Q)/\Delta f$
1.62542	1.62462	-0.0008	-8.00E-04	1.77E-02	2.41E+01
1.63618	1.63351	-2.67E-03	1.04E-02	3.84E-04	3.89E+00
1.6538	1.64915	-4.65E-03	1.70E-01	1.70E-01	3.65E+01
1.67692	1.67093	-5.99E-03	6.54E-02	2.86E-03	1.09E+01
1.70135	1.69639	-4.96E-03	1.98E+00	1.72E+00	3.99E+02
1.72236	1.72297	6.10E-04	4.29E+00	5.43E+00	8.90E+03
1.74938	1.75148	2.10E-03	4.88E+00	4.23E+00	2.32E+03
1.78046	1.78125	7.90E-04	4.44E-01	3.10E-01	5.63E+02
1.79854	1.80119	2.65E-03	9.32E-01	8.92E-01	3.52E+02
1.84182	1.84157	-2.50E-04	3.17E-02	3.33E-02	1.33E+02
1.8599	1.85919	-7.10E-04	2.04E+00	1.76E+00	2.87E+03
1.88807	1.88879	7.20E-04	4.03E-02	1.47E-01	2.04E+02
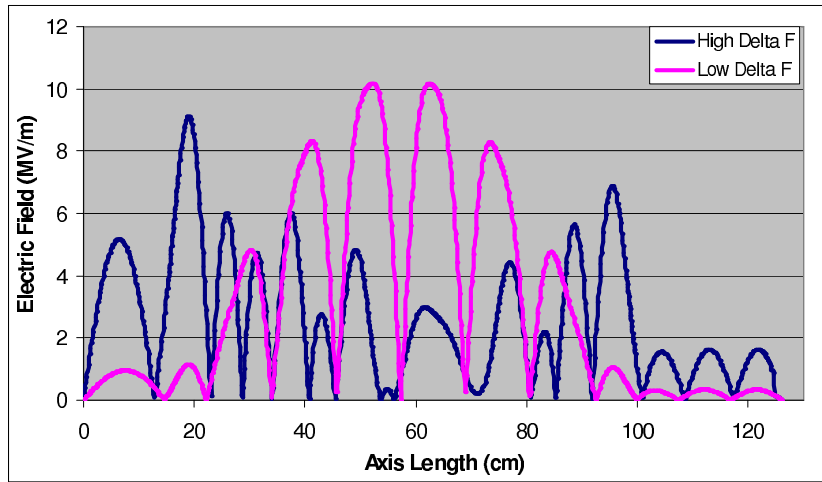
FIG. 4: Axis Electric Field Comparison, Lower and Higher Delta F

TABLE IV: CLANS2 Quadrupole Similar Frequency Mode Comparison, Odd vs. Even Symmetry Bound

$f_2[GHz]$	$f_3[GHz]$	$\Delta f[GHz]$	$R/Q_2[ohm/cm^4]$	$R/Q_3[ohm/cm^4]$	$max(R/Q)/\Delta f$
2.29958	2.29954	-4.00E-05	1.96E-02	1.85E-02	4.90E+02
2.30224	2.30198	-2.60E-04	5.94E-02	5.49E-02	2.29E+02
2.30613	2.30677	6.40E-04	1.81E-02	1.01E-02	2.82E+01
2.31055	2.31094	3.90E-04	2.01E-03	2.34E-03	6.00E+00
2.31478	2.31506	2.80E-04	4.18E-03	4.04E-03	1.49E+01
2.31824	2.3184	1.60E-04	3.91E-04	4.96E-04	3.10E+00
2.32053	2.32058	5.00E-05	5.20E-04	5.59E-04	1.12E+01
2.4725	2.47205	-4.5E-04	3.50E-03	3.29E-03	7.78E+00
2.4725	2.47205	-4.5E-04	350E-03	3.29E-03	7.78E+00
2.48447	2.4838	-6.7E-04	2.19E-03	2.61E-03	3.89E+00
2.48824	2.4891	8.6E-04	1.49E-02	1.36E-02	1.73E+01
2.49072	2.49085	1.3E-04	5.42E-02	5.20E-02	4.17E+02

III.   CENTER CELL OPTIMIZATION

As shown by introduction equation (7), the goal of the center cell optimization is to maximize $R/Q \cdot G$ for different iris radii to minimize fundamental mode losses - I optimized for 4 different iris radii: 30mm, 35mm, 39mm, and 43 mm. This optimization has two boundary conditions: angle of the tangent line between the two ellipses (see figure 1), and peak surface electric fields. The tangent angle must be less than 90 degrees to ease cleaning of the cell[5]). For my calculations, I chose the value of 82 degrees. Field emission, and thus power emitted, increases exponentially with peak surface electric field. I chose to look at two different field points as compared to the TESLA shape peak fields: $E_{pk}/E_{TESLA} < 1.1, 1.2$.

To run these optimizations, I designed a sequence of 3 programs. The first program defines the ranges of changes in the ellipse radii of the trial cells from the baseline (TESLA) shape and calls the other two programs for each trial cell. The second program then takes in a set of changes in ellipse radii from the baseline shape, calculates the tangent line to these ellipses, creates a geometry file of the cell for use in the 2D SRF simulation program CLANS, runs CLANS, and returns the difference between the fundamental frequency produced and the design goal of 1.3GHz. This input is the used as a non-linear function for the a MATLAB optimizer to find the optimum equator radius for each shape so that the frequency will be within 1kHz of 1.3GHz. Once the optimizer has tuned the cell frequency, the last program is called. This program takes the cell shape parameters and runs CLANS one last time, outputting R/Q, $R/Q \cdot G$, fundamental mode frequency, tangent angle, peak electric field, and peak magnetic field. [1]

In an attempt to verify my results, Professor Liepe calculated all 8 optimized shapes with a computer optimizer (instead of my hand-picked points) that used my program as a base and was based on $R/Q \cdot G$, a given peak electric field, and a given tangent angle of 82 degrees. Due to computer usage restrictions, Professor Liepe's optimizer produced the 30mm optimized shapes in my result table. We achieved very similar results, evidenced by the (nearly) smooth paramter curves that we both found (figures 8 and 9). The changes in radii are measured from the ellipse radii of the baseline cavity. These curves could be used to predict the optimal points for new values of iris radius.

The scan in cell shape parameters allows me to find the best points for a given iris radius and peak field (10 or 20 percent increase compared to the TESLA shape). To illustrate the effect of the tagential line angle on the achievable $R/Q \cdot G$, figure 5 shows points with red crosses through them for tangent angles less than 82 degrees, and the blue circles for tangent angles greater than 86 degrees. It can be seen that for a given peak electric field, increasing the tangent angle increases the maximum $R/Q \cdot G$. Also, for a given angle, $R/Q \cdot G$ increases linearly with peak electric field. I first use these programs to make a general plot with parameters in the general direction specified by Valery Shemelin and Sergey Belomestnykh[9]. I learned from observation how a change in each radius affected the points on the graph:

As you can see in figure 6, increasing A moved points up in R/Q*G but also in peak field, decreasing B moved in a similar direction to increasing A but with less for the same amount of change, decreasing a had a similar effect to increasing A, and decreasing b increased R/Q*G and decreased peak fields - an ideal combination as long as the radius does not

---

[1] All of these programs use the program "EllipseTangent" by Chad Parker to calculate the coordinates of the line tangent to both ellipses.
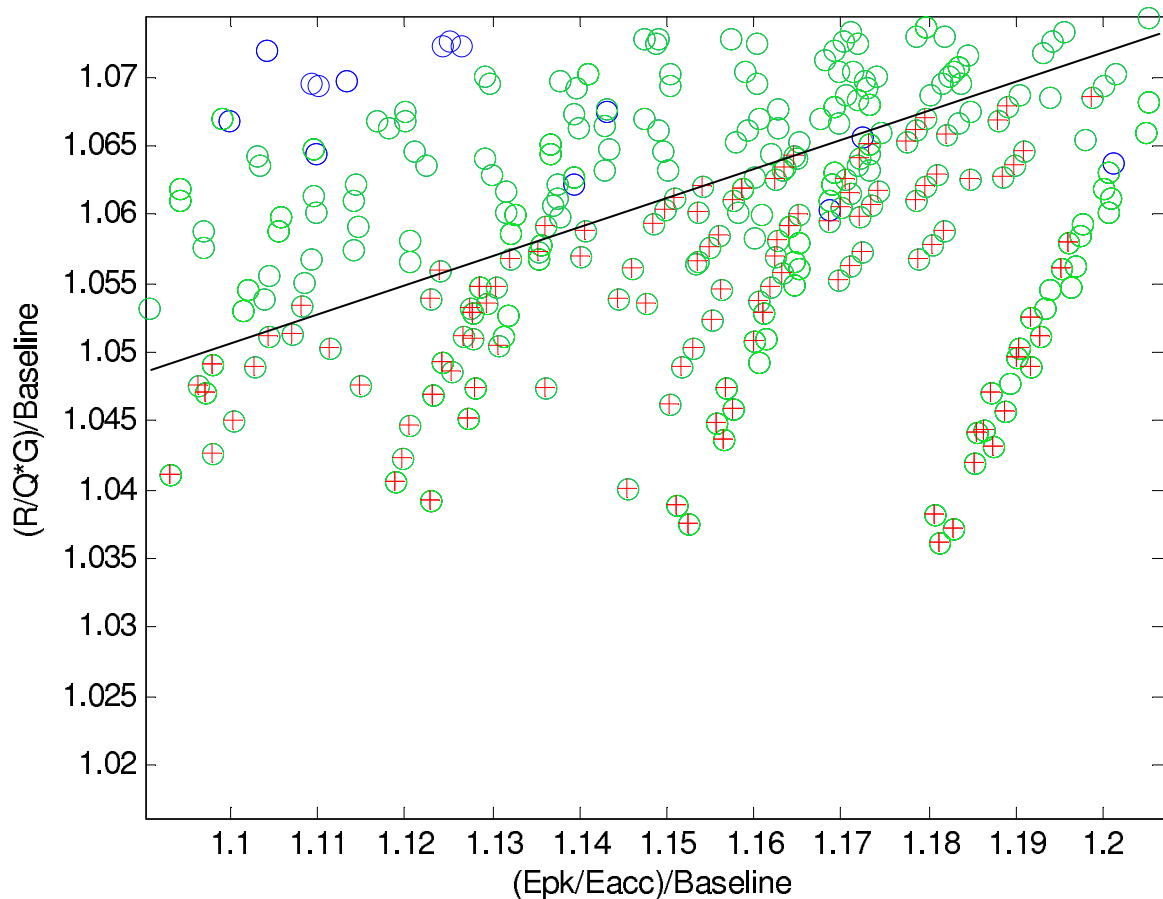
FIG. 5: (35mm Iris Radius), Cell Parameter Results for Points After General and Fine Scans

get too small. Changing a and b had a stronger effect than changing A and B because the peak surface fields occur near the iris. A and B compensate for each other, allowing for many combinations of A and B to produce the same $R/Q \cdot G$ value - however, each of those combinations will have a different tangent angle, which makes a wider range of tangent angles available. After looking at the general scan, I would decide how to change my parameters to end up on the "line" of 82 degrees at either 10 or 20 percent. Then, I would run as many detailed scans as needed to produce a satisfactory result. Finally, the optimal point would be reached - I aimed for an accuracy of 0.5 mm, because any smaller changes only changed R/Q and the field by only tenths of a percent.

This process produced 8 optimized cell shapes. Figure 7 demonstrates the geometrical differences between each cell. Table V shows all of the geometry data for each optimized cell as well as the baseline. Figures 8 and 9 show that the optimum points for a given lie on a smooth curve - this shows consistency in the results. The 35mm iris radius, 20 percent field seems to be a bit off of the curves for B and b.

I determined which cell would lose the least total power from Higher-Order Modes (HOMs) and the fundamental mode. I used the program NOVO, written by Alexander Novokhatski, to calculate loss factors for the shapes. I estimated power losses for a 7-cell cavity by multiplying the fundamental mode losses by 7 and by running NOVO for a cavity comprised of 7 copies of the optimized center cell. The fundamental mode losses can be multiplied by 7 because the power lost involves taking an integral over the surface of the
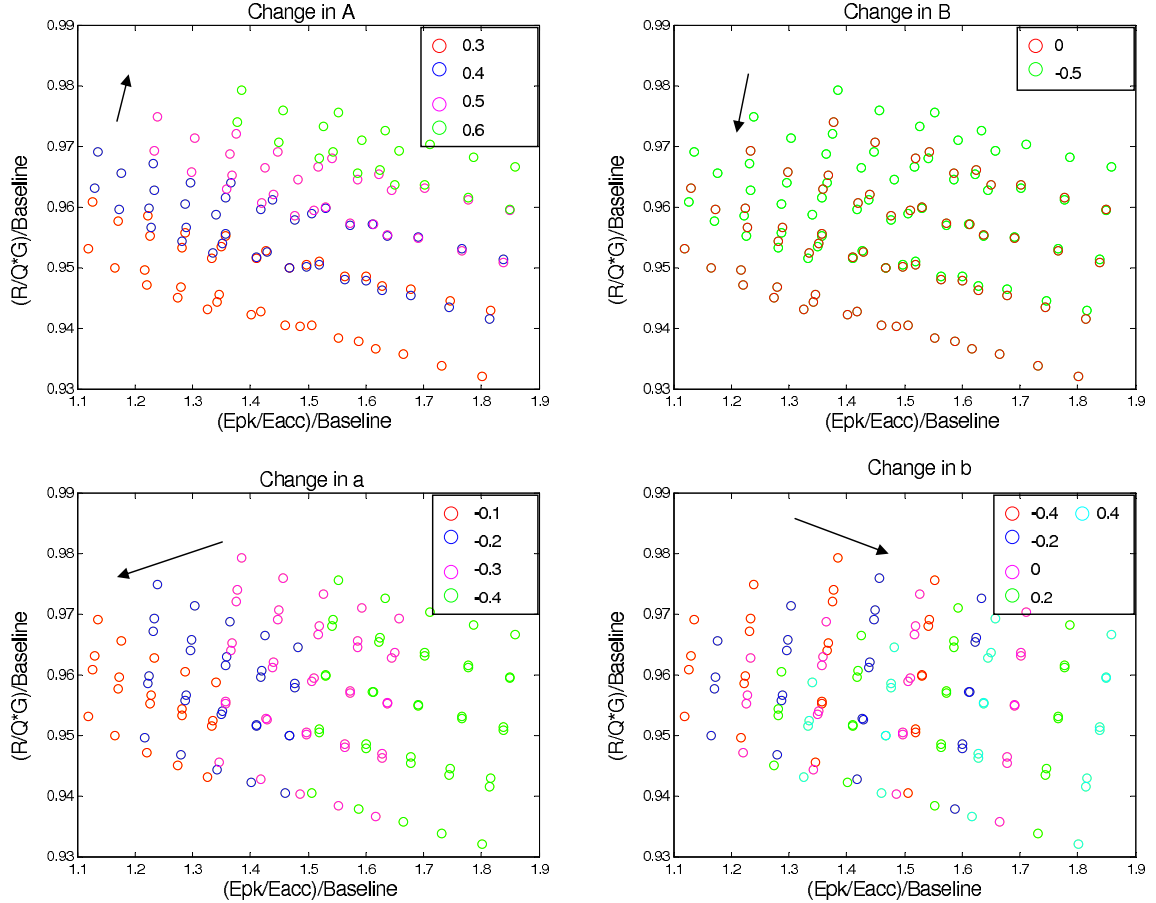
FIG. 6: Cell Dimension Changes, 39mm Iris Radius - Points with same color indicate cells with one same shape parameter, different values for other parameters

TABLE V: Geometry Data, 8 Optimized Center Cells

$r_{iris}[cm]$	E-Field Increase[%]	A[cm]	B[cm]	a[cm]	b[cm]	Height[cm]	$R/Q \cdot G[\Omega^2]$	Epk/Eacc
base (3.5)	0	4.2	4.2	1.2	1.9	10.33	15060	2
3.0	10	4.6	4	0.8	0.9	10.06	17763	2.20
3.5	10	4.5	3.8	1	1.3	10.16	15862	2.18
3.9	10	4.4	3.7	1.15	1.6	10.29	14324	2.20
4.3	10	4.2	3.6	1.4	1.75	10.43	12803	2.19
3.0	20	4.69	3.26	0.63	0.73	9.94	18094	2.41
3.5	20	4.6	3.85	0.85	0.85	10.15	16093	2.39
3.9	20	4.55	3.7	0.95	1.2	10.26	14564	2.39
4.3	20	4.45	3.7	1.1	1.3	10.41	13161	2.37

cavity. A surface integral over 7 of the same shape is the same as 7 times the integral over 1 of that shape. The loss factor for each optimized shape is shown in table VI.

For both 7-cell and 1-cell cavities, the loss factor increased as $1/r_{iris}$, verifying equation (10). The differences in loss factor between 30mm radius points is caused by larger geometry differences in the iris ellipses.
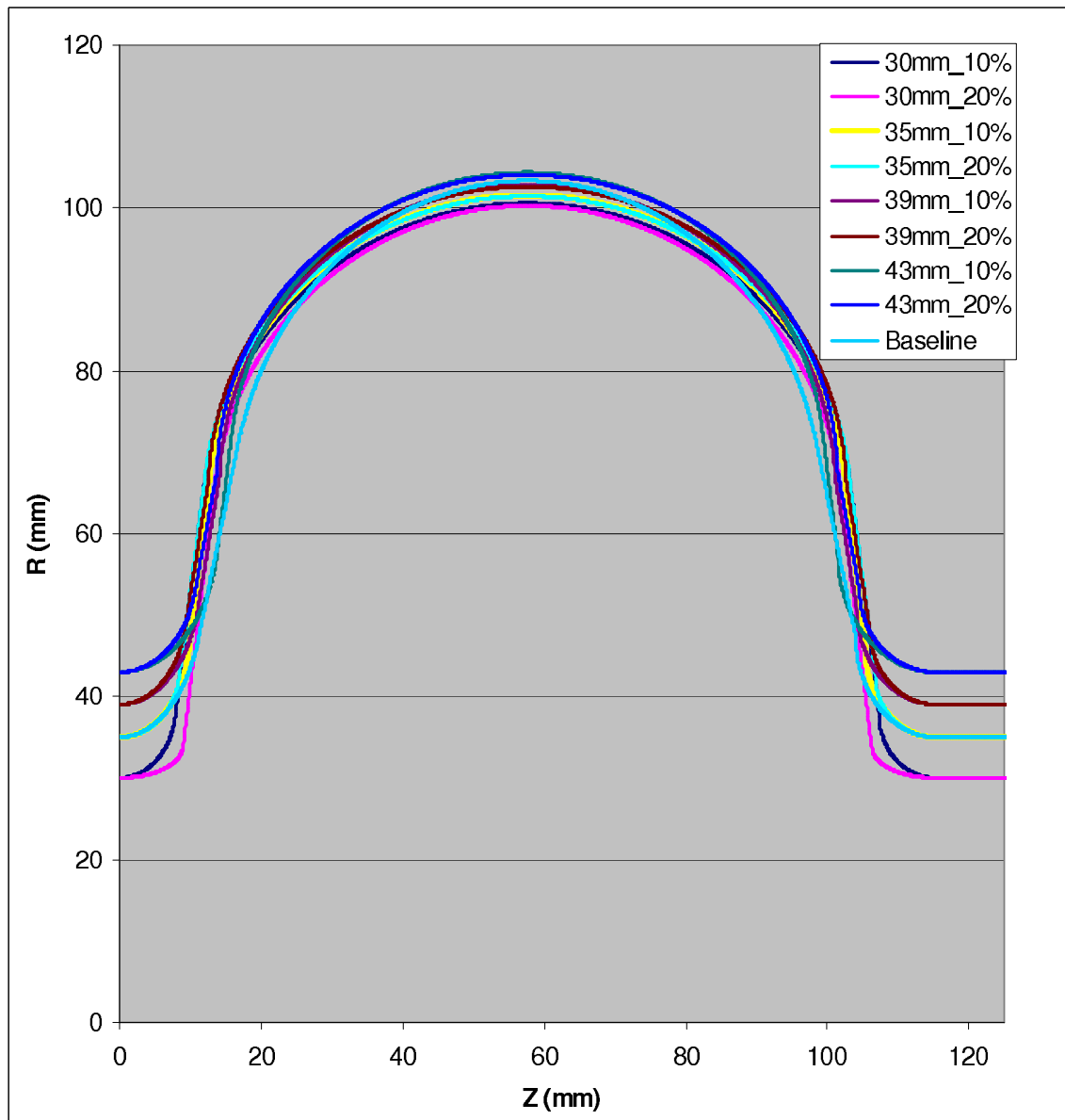
FIG. 7: Shape Comparison of 8 Optimized Cells and Baseline

I compared the sum of fundamental mode and HOM power losses in all 8 cavities in order to choose the best design. The power losses can be seen in table VI and in figures 12 and 13. The best cavity design is the 35mm iris radius, 10 percent field increase point. The 35mm shape was chosen over the 30mm shape because the small increase in power losses is compensated for by the capability of a bigger radius tube to better propagate HOMs out of the cavity. The 10 percent increase point was chosen over the 20 percent increase point because the benefit of an additional saving of 0.93 percent is small compared to the risk of increased field emission.
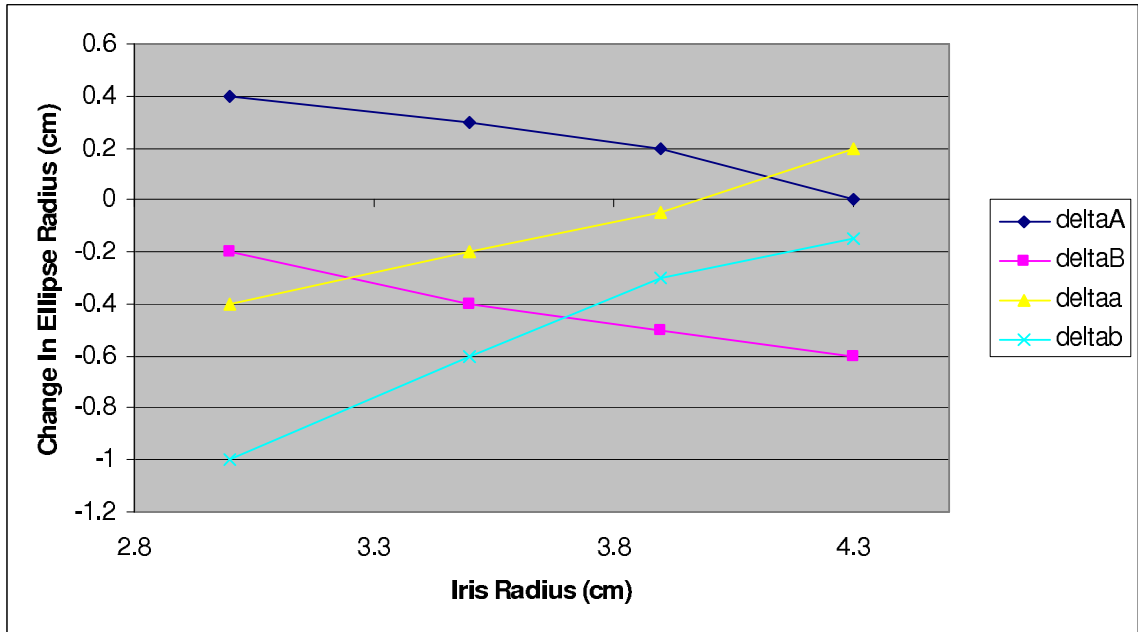
FIG. 8: Parameter Changes for Optimized Points vs. Iris Radius, 10 Percent Field Increase
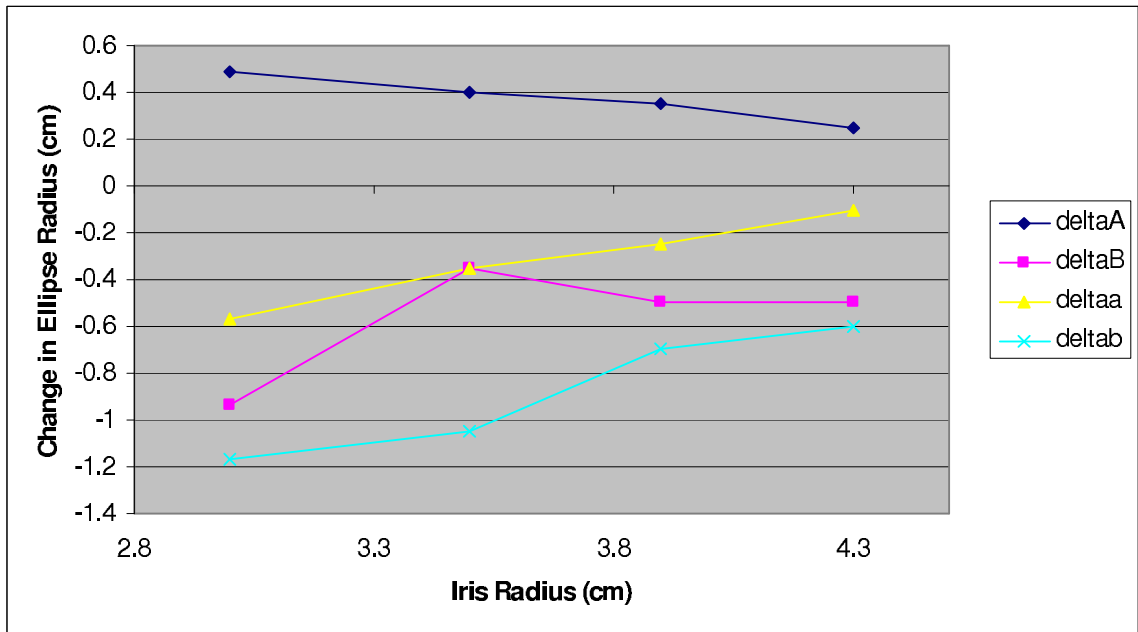
FIG. 9: Parameter Changes for Optimized Points vs. Iris Radius, 20 Percent Field Increase
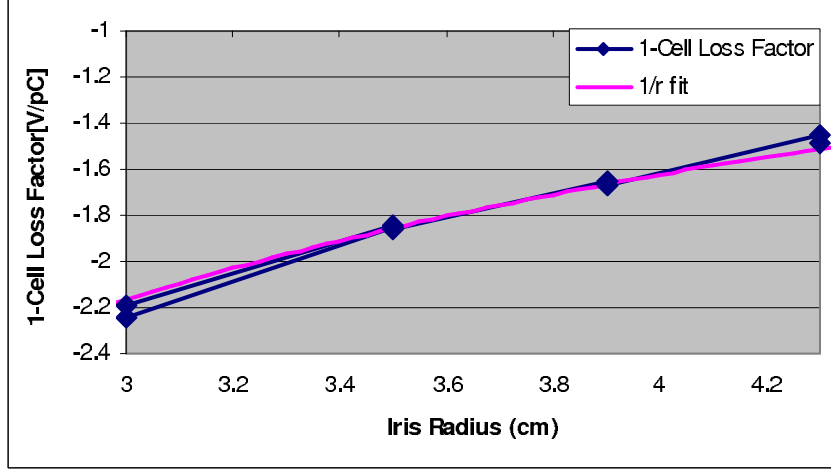
FIG. 10: 1-Cell Loss Factor vs. Iris Radius
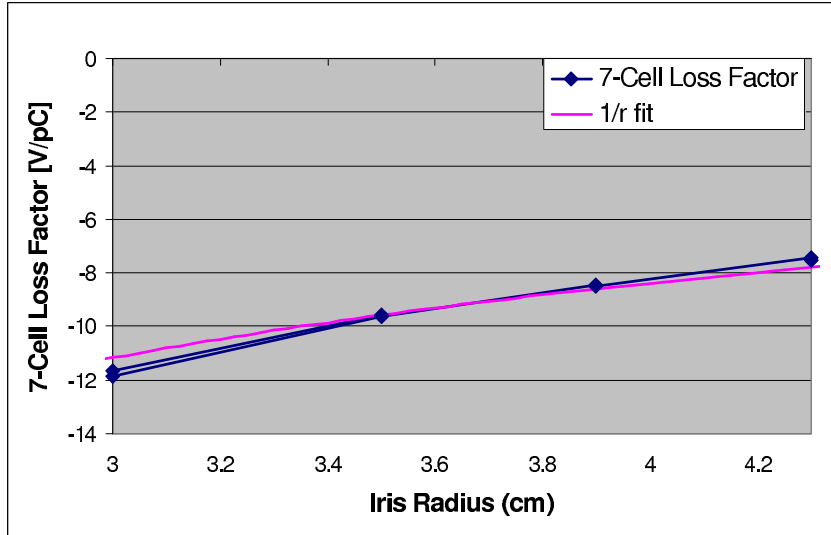
FIG. 11: 7-Cell Loss Factor vs. Iris Radius

TABLE VI: Power Comparison, 8 Optimized Center Cells

$r_{iris}[cm]$	Electric Field Increase[%]	K[V/pC]	7-cell K[V/pC]	$P_{hom,7}$[W]	$P_{fm,7}$[W]	$P_{tot,7}$[W]
base (3.5)	0	-1.841	-9.574	3686	8418	12104
3.0	10	-2.192	-11.667	4492	7137	11629
3.5	10	-1.856	-9.624	3705	7992	11697
3.9	10	-1.648	-8.436	3248	8850	12098
4.3	10	-1.455	-7.423	2858	9902	12759
3.0	20	-2.244	-11.848	4562	7006	11568
3.5	20	-1.859	-9.630	3707	7877	11585
3.9	20	-1.671	-8.507	3275	8704	11980
4.3	20	-1.487	-7.522	2896	9632	12528
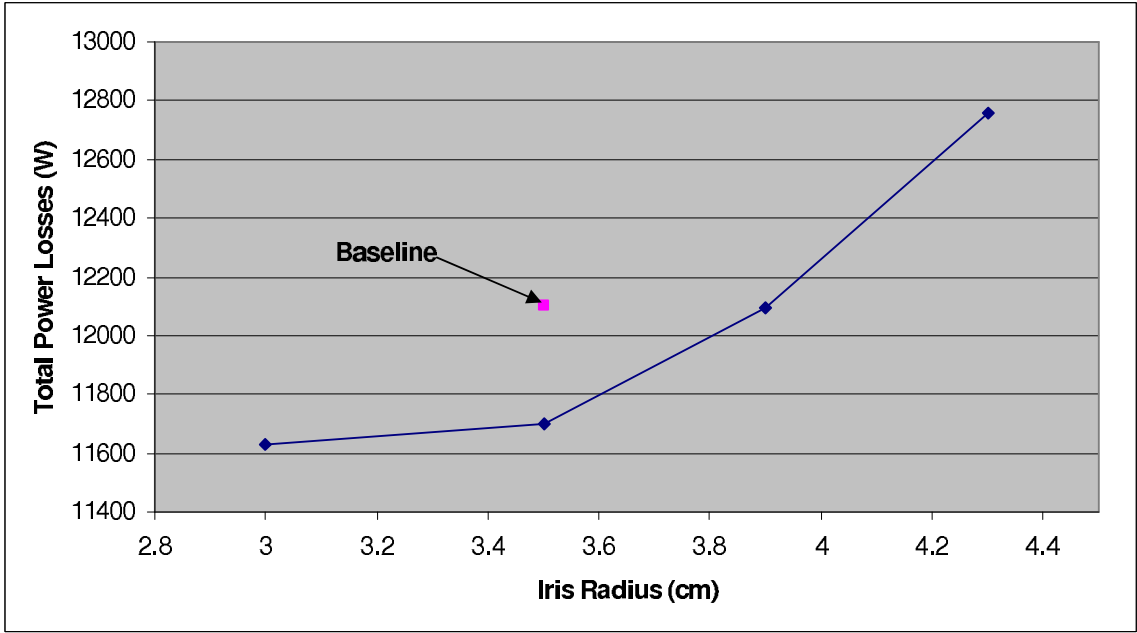
FIG. 12: 10 Percent Field Increase Power Comparison
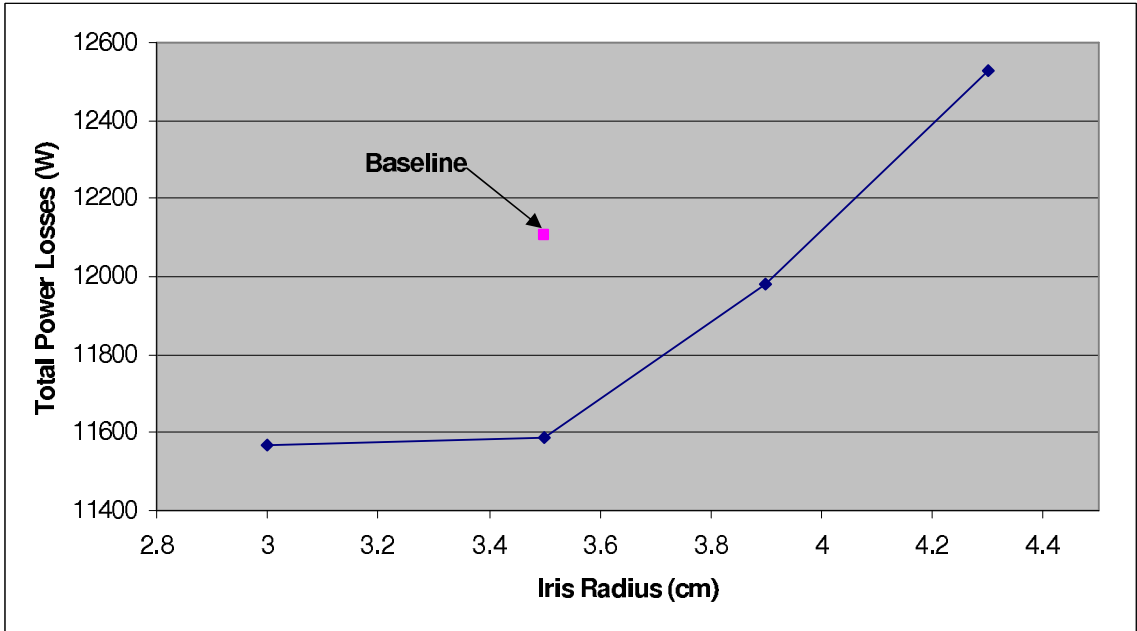
FIG. 13: 20 Percent Field Increase Power Comparison

IV. STARTING THE END CELL OPTIMIZATION

With an optimized center cell finished, I began work on finding optimized end cells for the 7-cell shape. The goal of this optimization is to avoid modes with low fields in end beam tubes, since these modes have the risk of having a high Q. These modes typically have a high R/Q and a frequency $f \approx N \cdot f_{res}$. For these modes, the goal is to minimize $R/Q \cdot Q$ as evidenced by the resonant HOM power loss and beam breakup equations (12 and 8). As set by the center cells, the boundary conditions of 10 percent peak electric surface field from the TESLA shape and tangent angle less than 82 degrees still apply.

I wrote a program to tune the accelerating mode frequency in the left and right end cells. For each end cell, I made a model including the beam tube, the outer end half cell, and two center half-cells. An example right end cell model is shown in figure 14. Since the cell height is fixed by the center cells, the length of the cell may be changed instead to set the frequency. Note that the geometries of the two end cells were significantly different because of the two different tube radii (65mm and 53mm) - one designed by Valery Shemelin[10] and one by Professor Liepe[5].
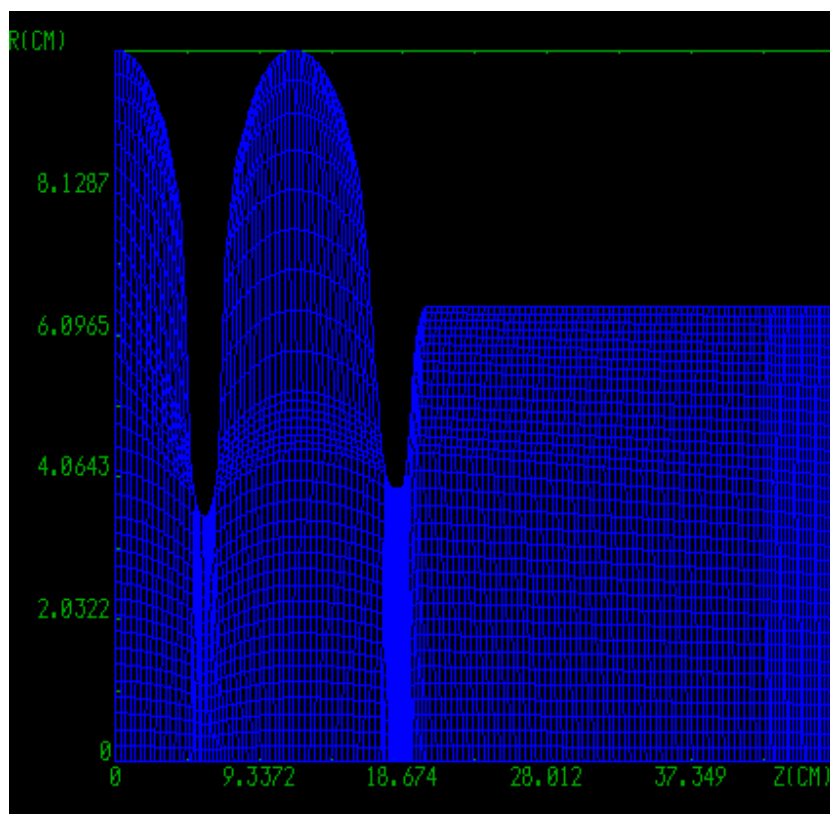

FIG. 14: Right End Cell Model With Solver Mesh

I wrote a program that produces a geometry file for the 7-cell cavity and runs CLANS or CLANS2 to find modes around a desired frequency. I set up tests to look at 2.6 and 5.2 GHz for monopole modes because they are low multiples of the 2-beam fundamental frequency 2.6 GHz, as well as at the lowest dipole modes. For these tests, I attempted to find the best combinations of $R/Q/\Delta f$ (to indicate the electric field in the tubes), peak electric field, and tangent angle. To use these programs, I ran a wide scan of possible ellipse radii where I

tuned the end cells to 1.3 GHz while measuring the tangent angle and peak electric field of the shapes. Then, the shapes with the best tangent angles (≤ 82 degrees) and peak fields ($\leq$ a 10 percent increase) were used with the 7-cell model and monopole modes testing to calculate $R/Q/\Delta f$. The sum of the $\frac{R/Q}{\Delta f}$ values of modes that appear in all shapes were calculated for 2.6 GHz and 5.2 GHz monopole modes in the right end cell and compared to produce a general model of an optimized end cell.
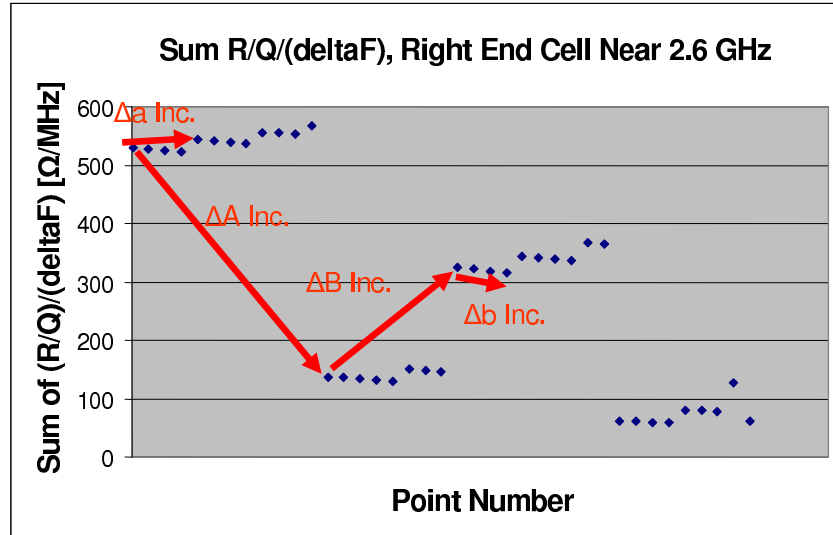
FIG. 15: Sum (R/Q)/Delta F, Right End Cell, Modes Near 2.6 GHz

As one can see in figure 15, the value changes exactly mirror changes in geometry, which suggests consistency in the data. For the first and last point on this graph, I compared the axis electric field profile of the mode that contributed 404 out of the roughly 500 Ω/MHz in the R/Q/Delta F value for the first point - see figure 16.
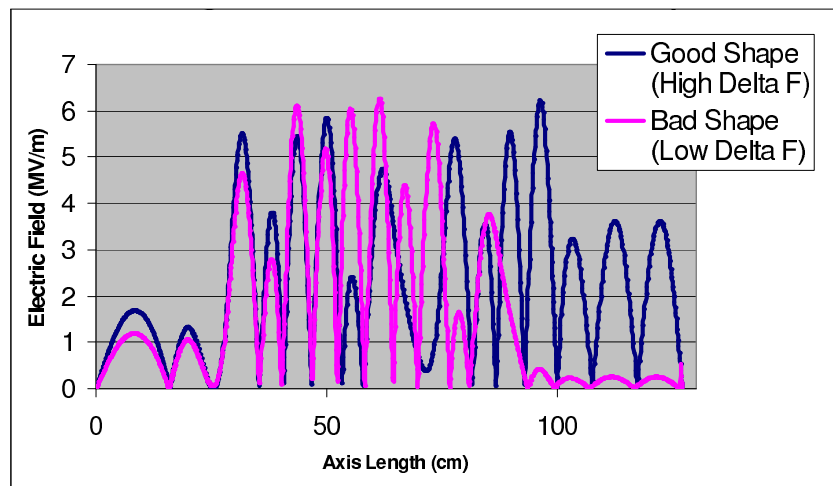

FIG. 16: Field Profile Comparison of Worst Mode around 2.6 GHz in First Point with Same Mode on Last Point in Figure 15

The electric field in the end cell (at $z \approx 95cm$) increases dramatically in the lower R/Q/Delta F point, again suggesting that high R/Q/DeltaF values indicate destructive

HOMs. This shows the important result that one can optimize mode propagation (field in the tubes) for the most dangerous modes by changing the shape of the end cell.

V. CONCLUSIONS

In this REU project, I found an optimized center cell for the proposed 7-cell superconducting RF cavities in the Cornell ERL Main Linac. This cavity shows a cryogenic loss improvement of 3.36 as compared to the baseline cavity. I also made significant progress on optimizing end cells for this cavity, and modeled a baseline cavity in Microwave Studio and CLANS. Future work on this project must start with analyzing general scans for left end cell designs, a "fine scan" for end cell optimum designs that takes dipole modes into consideration, and the development of a strategy for combining optimum left and right end cells. Related projects could include more 3D simulations of the optimized 7-cell cavity connected to HOM loads and studies to determine an ideal tangent angle parameter to use in place of the assumed 82 degrees in this project.

VI. ACKNOWLEDGMENTS

[1] Padamsee, Hasan. *RF Superconductivity for Accelerators.* John Wiley and Sons, Inc., New York, 1998.

[2] C.Pagani et al. for the picture of a half cell outline.

[3] G.H. Hoffstaetter et al., ERL Upgrade of an Existing X-Ray Facility: CHESS at CESR, Proceedings of EPAC 2004, Lucerne, Switzerland, (2004).

[4] Microwave Studio Software, CST Company

[5] M. Liepe, private communication.

[6] Zotter, Bruno; Kheifets, Semyon. *Impedances and Wakes in High-Energy Particle Accelerators.* World Scientific Publishing Co. Pte. Ltd., Singapore, 1998.

[7] G. Hoffstaetter and I. V. Bazarov, "Multi-Pass Beam-Breakup: Theory and Calculation", Proceedings of EPAC, Lucerne, Switzerland, 2004.

[8] H.Wang, R. Rimmer and G. Wu, "Elliptical Cavity Shape Optimization for Acceleration and HOM Damping",Proceedings of PAC, Knoxville, Tennessee, 2005.

[9] S. Belomestnykh and V. Shemelin, "High-beta Cavity Design - A Tutorial", Presented at SRF International Workshop, Ithaca, New York, 2005.

[10] V. Shemelin et al., Dipole-Mode-Free and Kick-Free 2-Cell Cavity for the SC ERL Injector, Proceedings of PAC 2003, Portland, OR, May 12-17, (2003).

[11] CLANS and CLANS2 Software Packages, Designed by D. Myakishev

[12] NOVO Loss-Factor Software, Designed by A. Novokhatski

[13] EllipseTangent MATLAB Program, Designed by C. Parker